Wick Irrigation Systems for Subsistence Farming

by

Lauren B. Kuntz

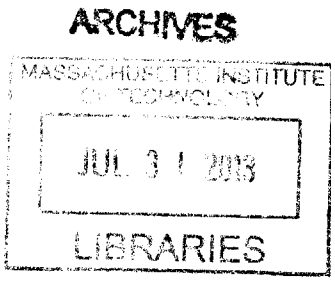

Submitted to the
in partial fulfillment of the requirements for the degree of

Bachelor of Science in Mechanical Engineering

at the

MASSACHUSETTS INSTITUTE OF TECHNOLOGY

June 2013

Author .....
May 10, 2013

Certified by .....
Amos Winter
Assistant Professor
Thesis Supervisor

Accepted by .....
Anette Hosoi
Professor of Mechanical Engineering

Wick Irrigation Systems for Subsistence Farming

by

Lauren B. Kuntz

Submitted to the
on May 10, 2013, in partial fulfillment of the
requirements for the degree of
Bachelor of Science in Mechanical Engineering

Abstract

Irrigation on small-scale farms has been noted as a key method to help lift subsistence farmers out of poverty. With water scarity growing around the globe and lack of access to electricity still prevalent in rural areas, the need to develop an energy efficient irrigation system that simultaneous limits wasted water while being low cost is essential. The possibility of using a wicking irrigation system that relies on the suction plants create for water to mitigate the pumping pressure is investigated. A theoretical model for such a system is developed for an acre sized wicking irrigation system, and the power and water efficiency is compared to a standard drip irrigation system. While the wicking irrigation system has a greater distribution of water delivery from the wicks than compared to the dripper system, a wicking system has the potential to operate at much lower power, with the possibility of even being a power source. If a direct coupling could be developed between the plant's roots and wick, eliminating the need for water to travel through the soil, the energy benefit of the wicking system would be even more dramatic.

Thesis Supervisor: Amos Winter
Title: Assistant Professor

Acknowledgments

I would like to express my deepest thanks to those who made this work possible. First of all, many thanks to Professor Amos Winter, who provided the vision and constant guidance for my thesis. In addition, thanks to Professor John Selker and Professor Amilcare Porporato for providing remote advice regarding wicking and modeling. For his help in lab and willingness to instruct me in regards to machining, I'd like to thank Dan Dorsh. To Jordan Mizerak, for being patient with my response to 'what are you working on?' constantly being 'my thesis,' I'd like to say thank you. Finally, I would like to express the greatest gratitude to Pawel Zimoch. Without your guidance, mentoring, and endless patience with my questions this thesis would not have been possible. Thank you all.

Contents

List of Figures

List of Tables

Chapter 1

The Problem

Over 800 million subsistence farmer around the globe rely on access to cheap water to grow crops. Through various irrigation methods, these farmers can increase their productivity and help alleviate poverty, yet with water supplies declining world wide, the importance of efficiently using water for irrigation is magnified. In addition, minimizing the systems energy consumption through optimization of water use and minimization of pumping pressure, is critical to keeping the operation costs low. To maintain the increased production and poverty reduction benefits associated with farmland irrigation, mitigating the system cost, pumping pressure, and water consumption will be essential in any irrigation system.

1.1 A Ladder Out of Poverty

Small-scale means of irrigation have been described as "a latter out of poverty" because irrigation increases yield, which increases income and food availability [14]. Irrigation provides both direct and indirect means of poverty alleviation. On the direct, localized level, irrigating crop lands increases production, providing farmers with greater access to food. At the same time, irrigation lowers the risk of crop failure, enabling farmers to transition to the growth of high-value, market-oriented

crops. This increased income is further supplimented by the ability of farmers to seek non-farm employment income, as irrigation lowers the daily time commitment for crop production [13].

In addition, irrigation acts through various indirect paths to help raise the community, as well as the farmer, out of poverty. Higher crop yields decrease the cost of food, allowing money to be spent through other avenues. This can help promote the development of other infrastructure in the community, which is further accelerated by the fact that governments and banks are more likely to provide funds for projects in areas with a high potential for success and growth [13].

1.2 Water Shortages

Over the past century, the rate of global water consumption has grown at more than double the rate of population growth, leading to an increase in regions with water scarcity. Today 1.2 billion people live in areas of physical water scarcity. By 2025, this figure is projected to increase to 1.8 billion living with absolute water scarcity, and over two thirds of the world's population facing water stressed conditions [4].

While there exists no global water shortage, the distribution of water is uneven - magnifying the water shortages for particular regions. In particular, India and regions of Africa, where a large number of subsistence farmers reside, are faced with water stresses and scarcity [4]. Especially in India, depletion of ground water resources is a major problem. The over development and withdrawl of wells has led to over a quarter of ground water blocks having reached semi-critical, critical, or overexploited levels. Unabated, this trend would lead to 60 percent of aquafers in a critical condition within 20 years. With over 60 percent of irrigated agriculture in India relying on groundwater sources, efficient and minimal use of water resources is essential. Access to water has a direct impact on poverty and food secruity for these farmers, and it is critical to minimize water wasted in irrigation to keep costs low and yield high [8].

1.3 Energy Efficiency

As of 2008, an estimated 1.5 billion people lacked access to electricity. Of those, 85 percent lived in rural areas predominately in Sub-Sahara Africa and South Asia - regions where subsistence farming dominates [7]. As electricity is necessary to power irrigation pumping equipment, regions with limited, intermittent, or no electricity access face difficulties in providing consistent and adequate crop irrigation. By decreasing energy and power requirements for irrigation, the barrier to electricity access and cost of running irrigation pumps would be mitigated. Should the system power be reduced significantly enough, it could be feasible to run irrigation equipment using a small solar cell, which would free the farmer from the cost and intermitency of the utilities network.

Chapter 2

Conventional Irrigation Systems

Over the past 50 years, the amount of irrigated land has nearly doubled, with currently 40% of the cropland irrigated in Asia alone [13]. While traditional methods of irrigation rely on gravity to provide the power for water movement, such as basin and furrow irrigation strategies, pressurize irrigation methods, including drip and sprinkler irrigation, rely on electricity to power the system. These pressurized irrigation methods have been growing in use due to their low labor requirement and high water efficiency. In particular, drip irrigation has grown in use for small, subsistence farms as a means of micro-irrigation [19].

A small 1-acre farm is modeled as a 60mx60m irrigation network, as shown in Figure 2-1. The backbone of the line connects to the pump, with $N = 120$ branches flowing perpendicularly from the line. Along each branch are $M = 120$ evenly spaced drippers, providing water to the plants. The systems flow parameters are taken to be representative of a typical small-scale, subsistence farm, and given in Table A.1.

For actual drippers, the flow rate of the dripper varies with the input pressure. Pressure compensating drippers are able to adjust internal pressure losses to maintain a constant flow rate over a given pressure range, enabling a uniform outflow over an irrigation system. Thus as pressure drops along the lines of the irrigation system, the drippers maintain a constant flow rate so all plants recieve the necessary amount of

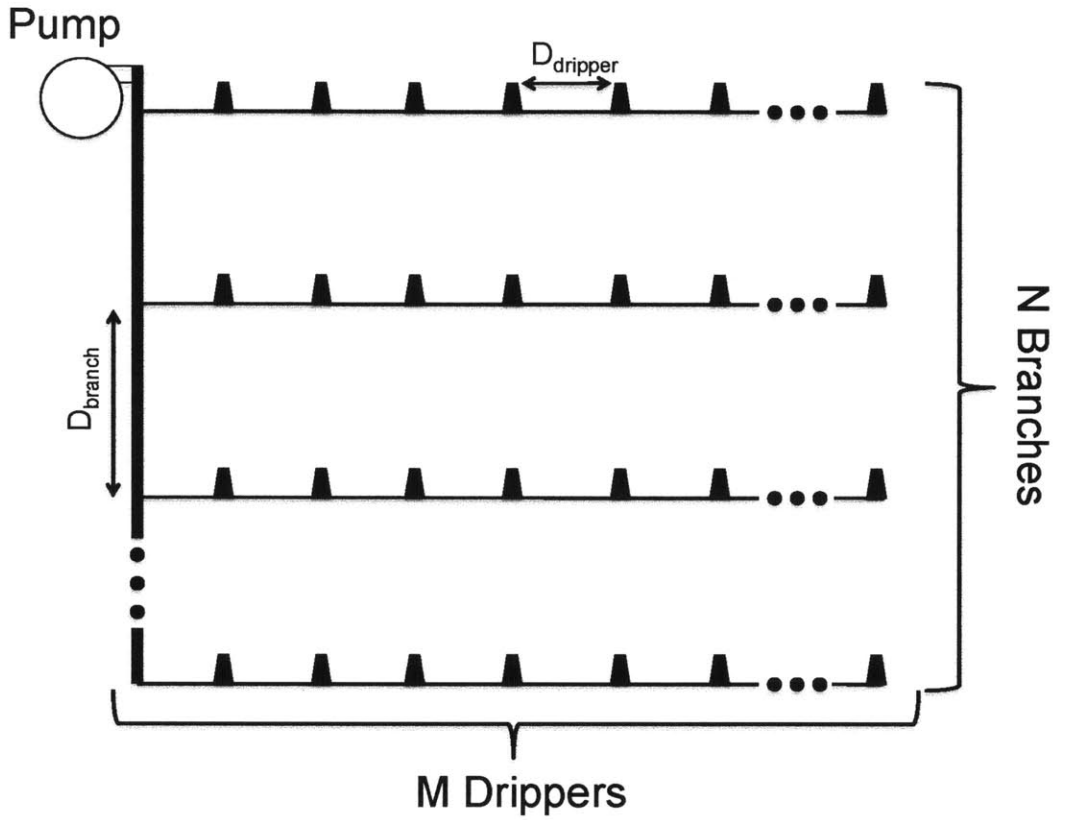

Figure 2-1: Diagram of $60m \times 60m$ irrigation system with one main line supplying $N = 120$ branches, each of which contains $M = 120$ drippers. The spacing between the branches and drippers is given by $D_{branch} = 0.5m$ and $D_{dripper} = 0.5m$ respectively.

water. In the ideal dripper case, the drippers are assumed to be perfectly pressure compensating, such that the flow rate is constant regardless of pressure head. The gauge pressure in the line at last dripper in the last branch is set as the boundary condition (with 0 MPa giving the setup with minimum input energy required), and the input pressure is calculated by backtracking the pressure losses, ΔP, along the pipe according to the Darcy-Weisbach equation

$$\Delta P = f \frac{L}{D} \frac{\rho_w V^2}{2} \tag{2.1}$$

where L is the length over which the pressure drop occurs, D is the pipe diameter, ρ_w

is the density of water, V is the average velocity of the fluid in the pipe, and f is the friction factor. There are a variety of empirically derived equations for f depending on the flow regime. For this model, the relation used for f is given by

$$f = 0.3164 Re^{-1/4} \tag{2.2}$$

for a Reynold Number Re [12]. Minor losses in pressure also result from the dripper and branch connections to the line. These losses are described as

$$\Delta P = \kappa \frac{\rho_w V^2}{2} \tag{2.3}$$

where κ is the minor loss coefficient that depends on the system geometry. Representative values of κ for branch junctions and drippers are given in Table A.1. For the case of the idealized dripper, shifting the gauge pressure of the final dripper just results in a net translation of the pressure profile of the system, as the flow rate is independent of absolute pressure level.

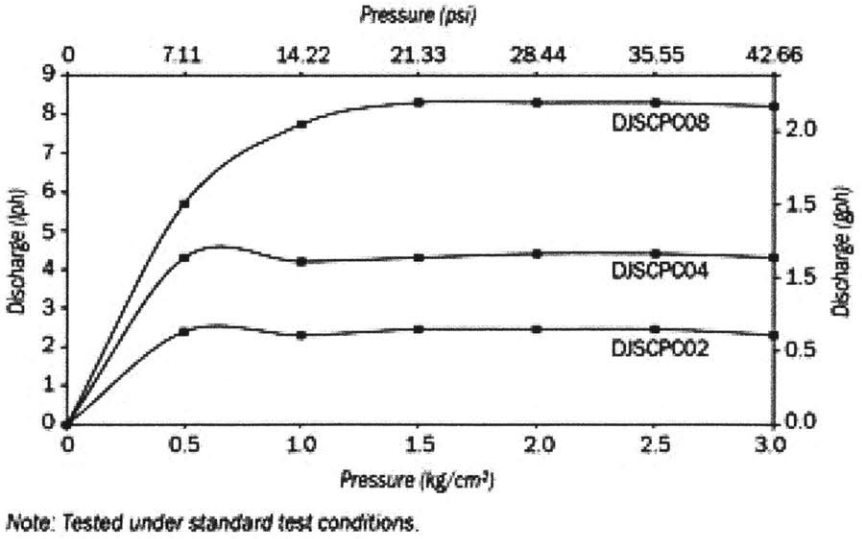

Figure 2-2: Measured flow rate as a function of input pressure for three types of Jain Irrigation Systems Ltd. pressure compensating drippers [3].

A more accurate description of dripper flow rate is obtained by modeling the dripper as an orifice. The inline drippers produced by Jain show orifice characteristics, with pressure compensation over a range of 1-3 atm, or about 0.1-0.3 MPa, and with a decrease in flow rate at lower pressures, as shown in Figure 2-2. The relation between flow rate and gauge pressure of these drippers can be described analytically with an error function:

$$\Delta Q = q_{max}\text{erf}\frac{P}{50,000Pa} \tag{2.4}$$

where ΔQ is the flow rate out of a given dripper, q_{dmax} is the maximum dripper flow rate, P is the pipe pressure in Pa, and 50,000 Pa is a scaling factor such that pressure compensation starts at $0.1MPa$. q_{max} is set such that all drippers operating at this flow rate over 8 hours would satisfy the irrigation requirement of 25,000 $\frac{L}{acre \cdot day}$, and the minimum operating pressure for the desired flow rate is 0.1 MPa. Figure 2-3 illustrates the relation between flow rate and pressure of the orifice dripper.

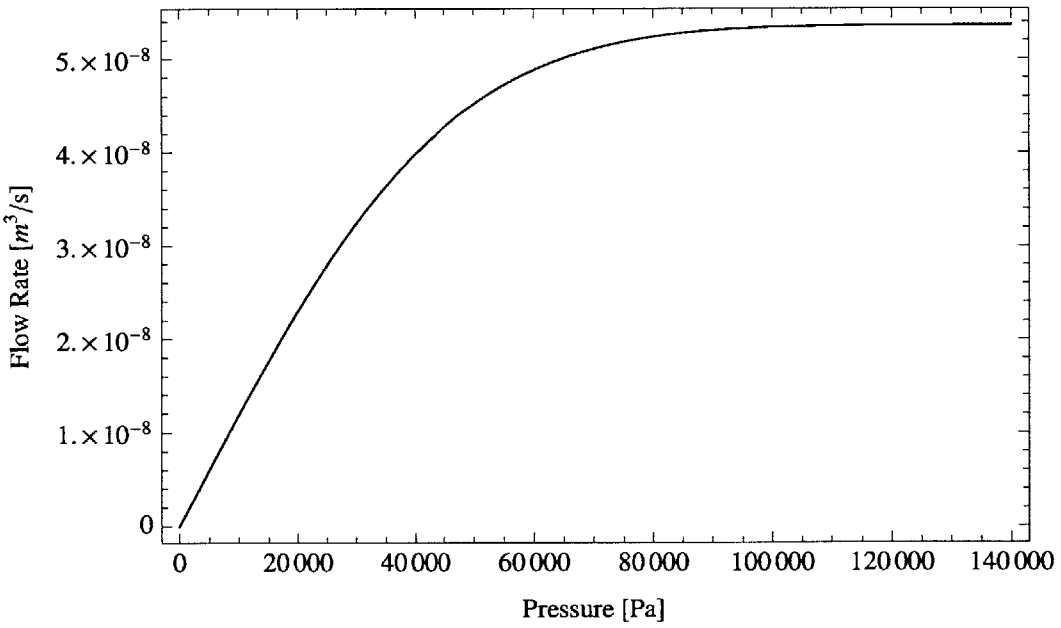

Figure 2-3: Flow rate as a function of input pressure for the model of the orifice dripper.

The system performance of the orifice model is determined by setting a desired input pressure and solving the Darcy-Weisbach equation for pressure losses along the main line and branches, and the orifice flow rate equation simultaneously. Increasing the input pressure of the system decreases the variance in dripper flow rate along the line, yet also results in an increase in energy demand. The Uniformity Coefficient, C_u, quantifies the presence of variation in the flow rate

$$C_u = 100\left(1 - \frac{\bar{\Delta q}}{q_{dripper}}\right) \tag{2.5}$$

Where $q_{dripper}$ is the desired dripper flow rate and $\bar{\Delta q}$ is the mean absolute deviation from $q_{dripper}$ [12]. Ideally, the flow would have no variation, such that each plant receives the same amount of water. As the amount of variation increases, a discrepancy between insufficient and excessive water arises, with some plants subjected to water stress, and wasted water for other plants.

The amount of power consumed by the system, P_{system}, is compared to the theoretical minimum power required to overcome the friction associated with pumping the water to the plants, P_{ideal}. P_{ideal} is determined for the idealized case with system parameters given in Table A.1. The required power to operate the system is calculated, and the power disipated over each of the drippers is subtracted to determine the ideal power necessary to overcome friction in the system. The efficiency of the system, η, is described as

$$\eta = \frac{P_{system}}{P_{ideal}} \tag{2.6}$$

Figure 2-4 shows the relation between the uniformity coefficient and energy efficiency of the idealized dripper and orifice systems. While increasing the pressure of the orifice system decreases the energy efficiency, it increases the uniformity coefficient. In the idealized dripper case, however, increasing pressure only serves to decrease the energy efficiency.

When looking at the possibility of using the wicking power of plants to promote

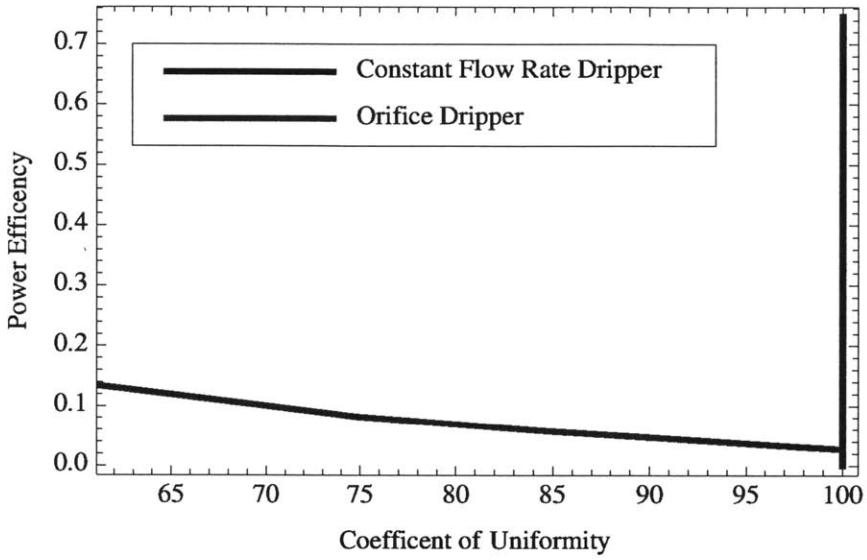

Figure 2-4: Comparison of performance of the ideal and orifice dripper systems for the 120 branch system with 120 drippers per branch. Additional system parameters given in Table A-1. The power efficiency is a measure of the neccessary power compared to the theoretical minimum power required to overcome friction, while the coefficent of uniformity is a metric to evaluate the variation of flow rates between drippers.

irrigation, the question is posed as to whether a system can be designed such that is requires less power, while still maintaining a high uniformity coefficient. If the power can be reduced enough, then it would be possible to use a small solar panel to power the system - eliminating the reliance on reliable access to electricity to power irrigaton. To ensure the plants still receive adequate water without unnecessary waste, however, it is vital that any wicking system would maintain a high uniformity coefficient. The goal is to design a system that falls to the top right of the spectrum in Figure 2-4.

Chapter 3

Fluid Flow in Soils and Porous Media

In order to describe the flux of water from a wicking irrigation system to the plants, it is essential to understand the flow of fluids in porous media. Equations for flux take on the general form of a gradient in potential providing the driving force with some measure of conductance or resistance regulating the rate. Ohm's law describing current driven by a difference in potential voltage, Fick's law for diffusion of a molecular species forced by a gradient in concentration, and Fourier's law of heat transfer through a material dictated by a temperature gradient are familar examples of fluxes. In the case of the movement of water through porous media, the driving force for flux is provided by a gradient in water potential.

3.1 Water Potential

Water potential describes the energy of water per unit volume, and is used to determine the direction of water flow in a system. Analogously to a ball rolling down a hill from a point of high gravitational potential to that of low potential, water will flow in the direction of minimum water potential. Water potential stems from the

chemical potential of water molecules, μ_w, with units of $\frac{energy}{mol}$

$$\mu_w = \mu_w^* + RT\ln a_w + V_w P + m_w g h \tag{3.1}$$

where μ_w^* is a reference potential, R is the ideal gas constant, T is the temperature in K, a_w is the chemical activity, V_w is the partial molal volume of water, P is the hydrostatic pressure in excess of atmospheric pressure, m_w is the mass, g is gravitational acceleration, and h is height relative to a reference level. The reference potential is taken to be pure water at standard temperature and pressure, with the gravitational level defined according to the system under consideration. Looking just at the gravitational term, this definition aligns with the analogy of a ball rolling down a hill given above. As the height of water is increased, it's chemical potential likewise increases, and the water would want to flow downward.

The chemical activity, a_w, is defined as the effective concentration of the water particles, and describes the likelihood of the particles to undergo a chemical reaction. The activity can be described as

$$a_w = \gamma_w N_w \tag{3.2}$$

where γ_w is the activity coefficient, and N_w is the mole fraction of water. γ_w takes into account the interaction of water molecules with interfaces, as the water molecules near interfaces are less likely to react in the bulk [18]. For clarity, the contribution to chemical potential due to the activity coefficient and concentration are separated

$$RT\ln a_w = RT\ln\gamma_w + RT\ln N_w. \tag{3.3}$$

Water potential, given in units of pressure, arises by comparing the chemical

potential to the standard potential and dividing by the molal volume:

$$\Psi_w = \frac{\mu_w - \mu_w^*}{V_w} = P + RT\ln\gamma_w + RT\ln N_w + \rho_w gh = \Psi_p + \Psi_o + \Psi_m + \Psi_h \quad (3.4)$$

where Ψ_p is the hydrostatic potential, Ψ_o is the osmotic potential due to presence of solutes in solution, Ψ_m is the matric potential that arises from capillary forces and interactions with interfaces, and Ψ_h is the gravitational potential [18].

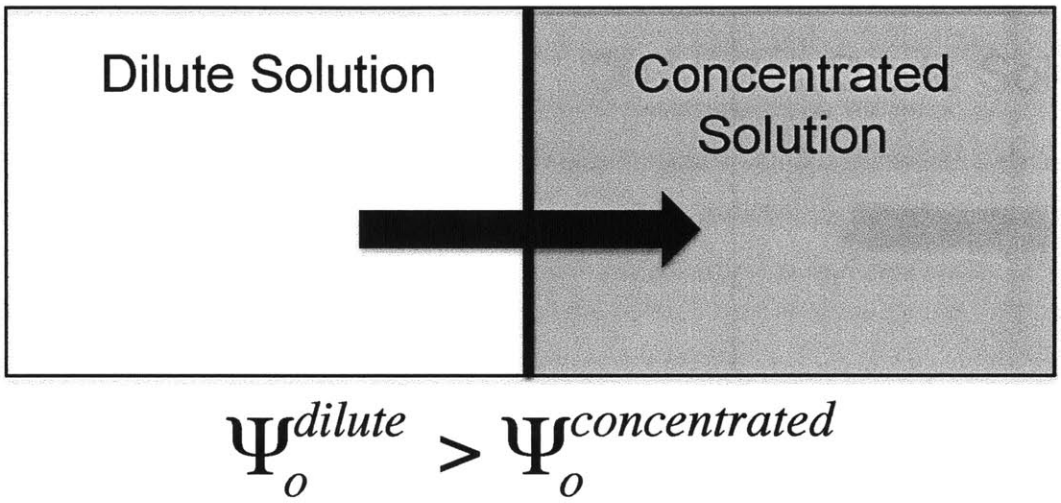

Figure 3-1: When a dilute and concentrated solution are separated by a semi-permiable membrane, the water will flow from the dilute to concentrated solution to counteract the difference in osmotic pressure. This flow is driven by a gradient in osmotic water potential.

While hydrostatic and gravitational potentials are familiar, osmotic and matric potentials are less customary. Osmotic potential stems from osmotic pressure created by the presence of solutes in solution. As we are familiar with in diffusion, a gradient in solute concentration will drive the flow of fresh water to counter act the concentration gradient, as shown in Figure 3-1. Matric potential arises from the combination of surface tension and adhesive forces between the fluid and surrounding surfaces that enables capillary action - the flow of liquid in small channels against the force of gravity. Capillary pressure, P_c, describes the pressure difference at the liquid's miniscus

and, in a porous media, is given by:

$$P_c = \sigma \left(\frac{1}{r_1} + \frac{1}{r_2} \right) \tag{3.5}$$

where σ is the surface tension, and r_1 and r_2 are the radius of curvature of the water surface and solid particle respectively as shown in Figure 3-2A. As the soil dries, the water recedes into the crevices between solid particles, decreasing the radius of curvature, and subsequently increasing the capillary pressure, as illustrated in Figure 3-2B. As such, a dry porous media exerts a higher capillary draw on water than wet one, and thus has a greater matric potential [9].

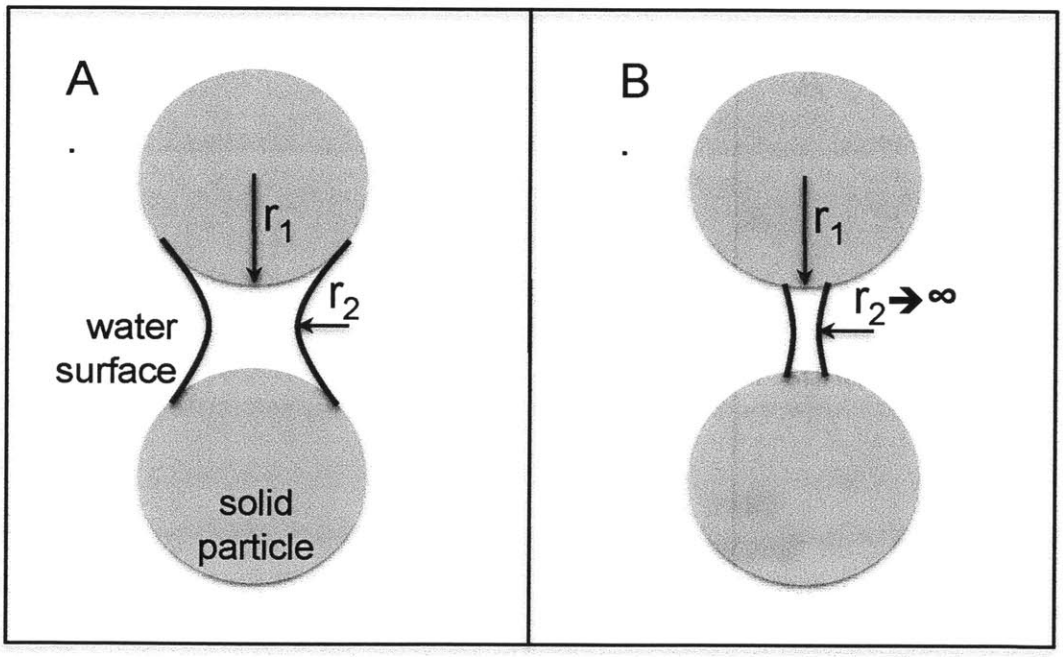

Figure 3-2: A. Two solid particles or radius r_1 generate capillary pressure in the water between them. B. As the water evaporates, the water surface receeds, increasing the radius of curvature of the interface, r_2, which results in an increase in capillary pressure.

3.2 Flux in Soil

The water potential in soil has combinations from each individual component - hydrostatic, matric, osmotic, and gravitational - that dictate the direction in which water will flow. While the gravitational component will cause a general downward flux of water into the soil, horizontal water flux is often dominated by differences in the matric potential of the soil. Generally, the osmotic and hydrostatic components are substantially less significant than the matric potential, which can exceed -1.5 MPa.

The matric potential of a soil depends on the level of saturation of the soil, as drier soils exert a stronger capillary draw on water than wet soils. Water retention curves, as shown in Figure 3-3, show the relationship between soil water content and matric potential. While water retention curves have the same general form, they are characteristic of each soil type and determined experimentally. These curves are described analytically by

$$\Psi_s = \bar{\Psi}_s s^{-b} \tag{3.6}$$

where Ψ_s is the water potential of the soil, $\bar{\Psi}_s$ is the saturated soil potential, s is the water content, and b is an experimentally determined exponent [10]. Values of these parameters for loamy sand used in the model are presented in Table A.2.

The flux of fluid through a porous media is described by Darcy's Law

$$q = -K\nabla\Psi_w \tag{3.7}$$

where q is fluid flux, and K is the hydraulic conductivity. As with the soil water potential, the hydraulic conductivity varies with water content, and is a characteristic of a given soil type. The hydraulic conductivity decreases with the water content of a porous media due to the occurrence of cavitation as the water potential drops and air gaps break the water connections within the soil [20]. As the soil dries, it becomes more difficult for water to flow. Experimental measurements of hydraulic conductivity

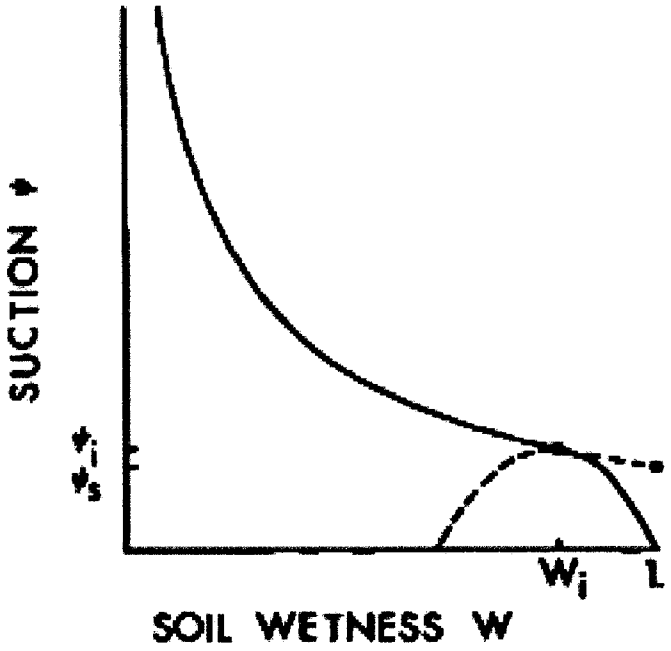

Figure 3-3: The water retention curve shows the relation between water content, W, and suction (note, suction is definite such that a positive value corresponds to a negative water potential). The curve is composed of a piecewise function, where for low water content the relation is hyperbolic, while for high water content, a parabolic fit is more appropriate. The dashed lines show the fits in the regions where they are not applied and are disregarded. For the purpose of this study, the hyperbolic fit is applied over the entire range of soil water content. Figure is taken from [10].

as a function of water content are described analytically by

$$K = K_{sat} s^{2b+3} \tag{3.8}$$

where K_{sat} is the hydraulic conductivity at soil saturation, and b is the same exponent as in equation 3.6 [11]. The saturated hydraulic conductivity for loamy sand used in the model is $K_{sat} = 100\frac{cm}{day}$, and is also given in Table A.2

Chapter 4

Fluid Flow In Plants

The flow of fluid from soil into plants is dictated by the gradient in water potential between the soil, roots, leaves, and air. Evaporation of water from the pores in the plant leaves, the stomata, into the air generates a tension that is transmitted along the plant. As water evaporates from the leaf, it increases the concentration of solutes, hence decreasing osmotic potential and the total water potential in the leaf. This lowered water potential drives the flux of water from the roots into the leaves. Figure 4-1 shows typical water potential values at various locations along the soil-plant-atmosphere continuum [18]. In addition, the conductivity of each component of the system describes the ease of fluid flow through the system and helps control the flux. Understanding the water potential and conductivity at each point throughout the soil-plant-atmosphere system is critical to determining the rate of water consumption by the plant.

4.1 Evapotranspiration

The gradient in water potential between the leaf and air provides the driving force behind evaporation of water. The water potential of the air arises from the relative humidity of the air. Evaporation of water into the atmosphere is favored since the

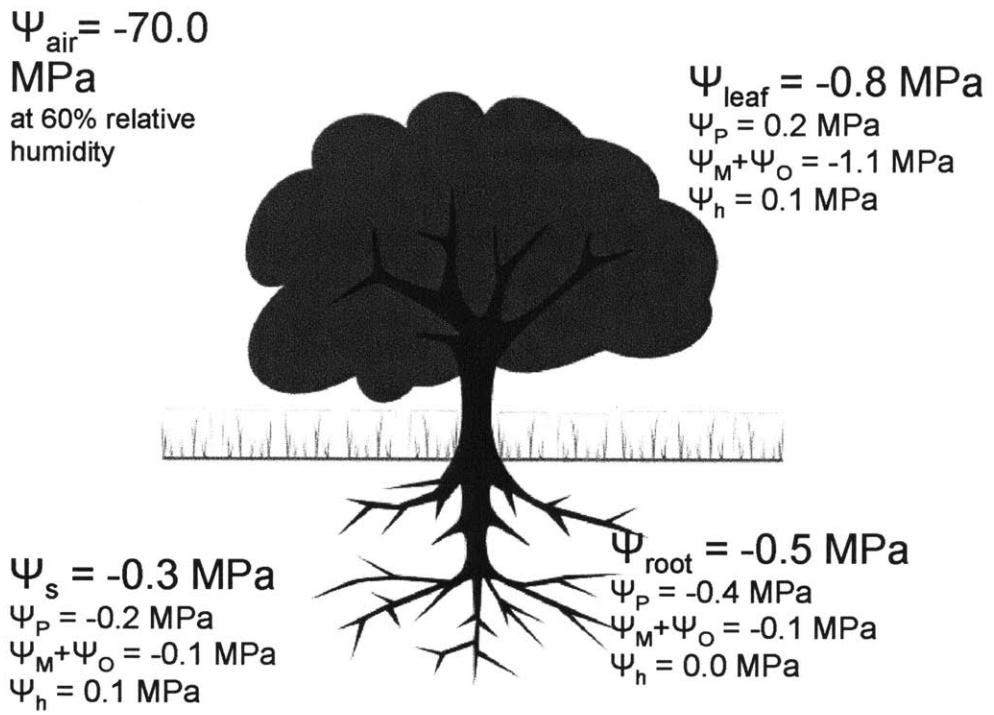

Figure 4-1: Representative values for the water potential of the various parts of the soil-root-plant-atmosphere continuum are shown along with the individual contributions from hydrostatic, osmotic, matric, and gravitational potential [18].

air is not saturated with water vapor, and hence not in equilibrium. Water potential in the atmosphere is governed by

$$\Psi_{wv} = \frac{RT}{V_w} \ln \frac{P_{wv}}{P^*_{wv}} + \rho_w g h = \frac{RT}{V_w} \ln \left(\frac{\%\text{Relative Humidity}}{100} \right) \tag{4.1}$$

where P_{wv} is the water vapor, P^*_{wv} is water vapor at saturation, and the ratio of the two is defined as relative humidity. The gravitational potential term is dropped, as elevation effects are negligible compared to those of relative humidity. The water vapor potential can have extremely large negative values, as small changes in relative humidity result in large changes in potential, as shown in Figure 4-2 for 20 C. At this temperature, a change from 99% relative humidity to 98% relative humidity results in the doubling of water potential from -1.36 MPa to -2.72 MPa [18].

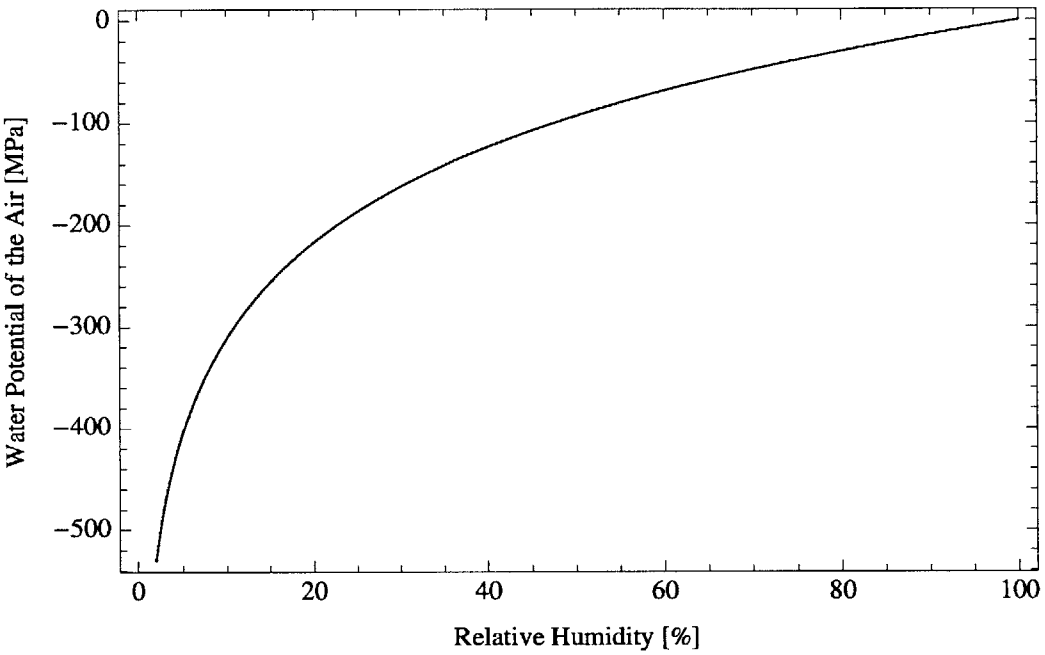

Figure 4-2: Water potential of the air is shown as a function of relative humidity. Initially, small decreases in relatively humidity from 100% result in small changes in water potential, but as the air gets farther from saturation, the potential drops rapidly.

Evaporation of water from the stomata is the primary source of water loss for plants, with the rate of transpiration being substantially larger than the rate of all of the other water uses in the plant combined. A small fraction of the water drawn by a plant is used in photosynthesis reactions and to enlarge cells and promote growth, but as evapotranspiration accounts for the vast majority of plant water use, a plants evapotranspiration rate is oftentimes assumed to be equivalent to adsorption rate [17]. Evapotranspiration through the stomata is essential, as these air-water interfaces enable for the flux of carbon dioxide into the plant, which is required for photosynthesis [18].

Solar radiation provides the energy behind plant evapotranspiration. Although the rate of water flux depends on local meteorological variables, such as temperature,

wind speed, and relative humidity, it can be approximated by the Penman-Monteith equation

$$EV_{plant} = \frac{\Delta\, R_n + \rho_a c_p \delta\, g_a}{\rho_w \lambda_v \left(\Delta + \gamma \left(1 + \frac{g_a}{g_s}\right)\right)} \tag{4.2}$$

where EV_{plant} is the rate of water flux per unit ground area, Δ is the rate of change of vapor pressure with temperature, R_n is the net irradiance reaching the leaf, ρ_a is the density of air, c_p is the specific heat of air, δ is the vapor pressure deficit from saturation, g_a is atmospheric conductance, λ_v is the latent heat of water vaporization, γ is a psychrometric constant, and g_s is the conductance of the plant stomata [11]. While many of these variables can be determined locally, representative values are taken to provide reasonable predictions of evapotranspirtation rates. Table A.3 provides the values and descriptions of the various variables used in the model.

The conductance of the stomata varies with leaf potential, and serves as the plants regulation system for evapotranspiration. The stomata can open and close in response to the environment to adjust the air-water interface area, and consequently the conductance, controlling the rate of evapotranspiration. If the rate of water loss exceeds the rate of water intake, the stomata can act as a negative feedback loop to preserve steady state by partially closing to minimize water losses (or opening further in the case where water intake exceeds water loss). The stomata conductance depends on a number of variables

$$g_s = g_{smax} f_\phi(\phi) f_T(T) f_{\Psi_l}(\Psi_l) f_D(D) f_{CO_2}(CO_2) \tag{4.3}$$

including irradiance, ϕ, air temperature, T, vapor pressure deficit, D, leaf water potential, Ψ_l, and carbon dioxide concentration, CO_2, where g_{smax} is the maximum stomatal conductance observed when none of the variables are limiting. For the purpose of this investigation, only the effects of leaf water potential are considered. Under well-watered conditions, the leaf potential is assumed to have no impact on stomatal conductance until a threshold value, Ψ_{lo}, is reached, at which point the stomata begin

to close. As the water potential decreases further, the stomatal conductance drops linearly to zero when the stomata fully close at the water potential of the wilting point, Ψ_{wilt} [11]

$$f_{\Psi_l}(\Psi_l) = \begin{cases} 0 & \Psi_l < \Psi_{wilt} \\ \frac{\Psi_l - \Psi_w}{\Psi_{lo} - \Psi_{wilt}} & \Psi_{wilt} \leq \Psi_l \leq \Psi_{lo} \\ 1 & \Psi_{lo} < \Psi_l \end{cases} \tag{4.4}$$

As the energy for evapotranspiration comes primarily from solar radiation, the system can be viewed abstractly as a solar cell. The average solar radiation hitting earths surface is 1361 $\frac{W}{m^2}$ [16], and solar cells work to convert this energy into usable electrical energy. The best reported efficiency of solar cells without solar concentration is 37.8%, achieved by Boeings subsidiary Spectolab [1]. By comparison, the evapotranspiration process in plants is up to 31% efficient in well-watered soils, but drops off as the leaf water potential decreases, as shown in Figure 4-3.

4.2 Soil, Root, and Plant Conductance

As seen with evapotranspiration in the stomata, conductance drops with water potential. Similarly, between the soil and roots, and throughout the plant, conductance drops as water potential decreases. This drop in conductance is largely due to the onset of cavitation that breaks the continuity of the water continuum [20]. The plant conductance, g_p, is modeled by a vulnerability curve

$$g_p = g_{pmax} \exp\left(-\left(-\frac{\Psi_l}{d}\right)^c\right) \tag{4.5}$$

where g_{pmax} is the maximum plant conductance observed for low values of Ψ_l, and c and d are fitted parameters. As the leaf potential drops, the plant conductance decreases to zero. The soil root conductance is described by

$$g_{sr} = \frac{K\sqrt{R_{AI}}}{\pi g \rho_w Z_r} \tag{4.6}$$

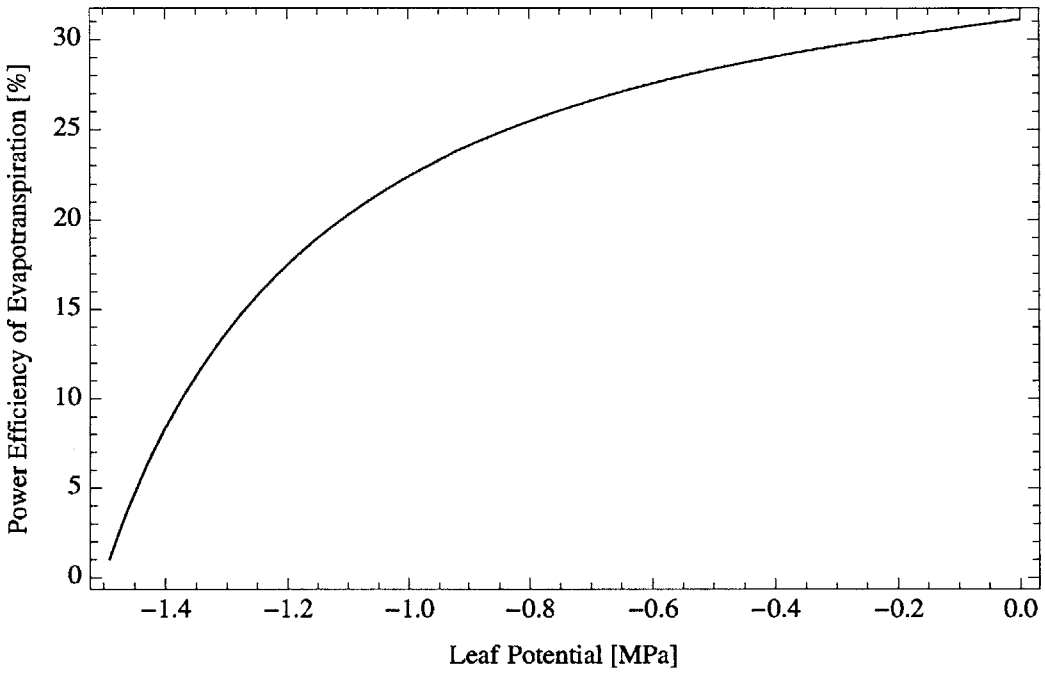

Figure 4-3: The power requirement for evapotranspiration is compared to the incoming solar radiation power which provides the energy behind fluid flow in plants to give power efficiency. The power efficiency is plotted as a function of leaf potential, and drops off as the leaf potential approaches the wilting point.

where K is the hydraulic conductivity of the soil given by equation 3.8, R_{AI} is the root area per unit ground area, and Z_r is the characteristic root length [11]. Representative values of these parameters are given in Table A.3.

Through the variation of conductance in the soil-plant-atmosphere continuum, the leaf water potential adjusts to changes in soil water content to maintain water flux through the system. As illustrated in Figure 4-4, as the soil dries, the water potential of the root and leaf drop accordingly to maintain the gradient in water potential necessary to drive the flux of water through the plant. Once the wilting point is reached, however, no lower leaf potential can be achieved as the stomata are fully closed. Generally, this permanent wilting occurs when Ψ_{soil} is around -1.5 MPa. At night, the potential of the soil, root, and leaf become essentially equal as stomata

close and evapotranspiration ceases [18].

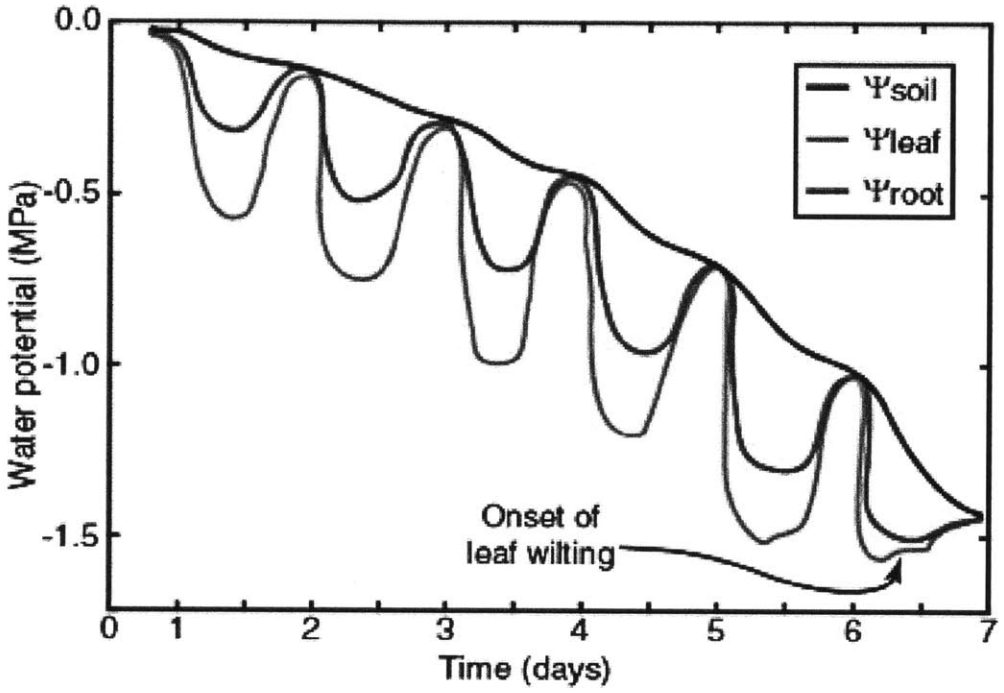

Figure 4-4: As the soil dries, the root and leaf potentials drop in response to maintain water flux through the plant. Eventually, the plant hits the wilting point, at which point it can no longer sustain an adequately negative potential to drive water flow. Note that during the night, when the stomata close, the potential of the soil, roots, and leafs equilibrate such that flow stops. Figure is taken from [5].

Looking at a plant in equilibrium with the soil, there is a trade-off between leaf potential and water flux through the system. Because hydraulic conductivity drops with leaf potential, water can not flow through the plant as easily. Hence, the flux of water decreases. Plants with higher leaf potentials have greater conductivity and flow rates, yet as water in the soil is more readily available, the roots generate less suction for water. When looking at the possibility of using a wicking system to irrigate crops, setting an equilibrium operating point with the lowest leaf potential of the plants would maximize the suction the roots can provide. At the same time, it would limit the amount of water the plants receive, possibly subjecting them to water stresses.

Any wicking irrigation system would have to balance adequate water flux with the plant's suction for water.

4.3 Fluid Flux in the Proximity of the Roots

The presence of a plant's roots in soil is generally felt over a distance on the order of 1 *cm* from the root, as this is the length scale between individual roots of a given plant. Beyond this distance, the soil is considered to be a bulk with constant potential and conductivity. An understanding of the water potential within the area immediately surrounding the root can be obtained by looking at the gradient required to sustain a constant flux. Describing the root as a cylinder with constant flux per unit length, and simplifying the soil hydraulic conductivity to assume a constant value, Darcy's equation can be used to determine the required potential gradient between the root surface and surrounding soil

$$J(r) = -\frac{K\nabla\Psi_{soil}}{\rho_w g r} ln\left(\frac{r_{root}}{r}\right) \tag{4.7}$$

where J is the volume of water uptake at the root surface per unit area, r is the radial distance from the root, and r_{root} is the root radius. Representative values are taken to be $1.1 \times 10^{-7}\frac{m}{s}$ for volumetric water flux per root area,$9.8 \times 10^{-12}\frac{m}{s}$ for the hydraulic conductivity of a loam soil with low water content, and 0.5 *mm* for the root radius. Using these representative values, the difference in potential between the root surface and soil 1 *cm* away is 0.16 MPa, and Figure 4-5 show a plot of the difference in potential between the root surface and soil as a function of radial distance [18].

Since the water potential decays as the inverse of radial distance, proximity to the root has a significant impact on the pumping power felt by the water source. In terms of energy efficiency of a wicking irrigation system, the closer the wick can be to the root, the greater the benefit of the tension generated by the plant. Ideally, the maximum pumping power from the plant would be felt by directly coupling the root

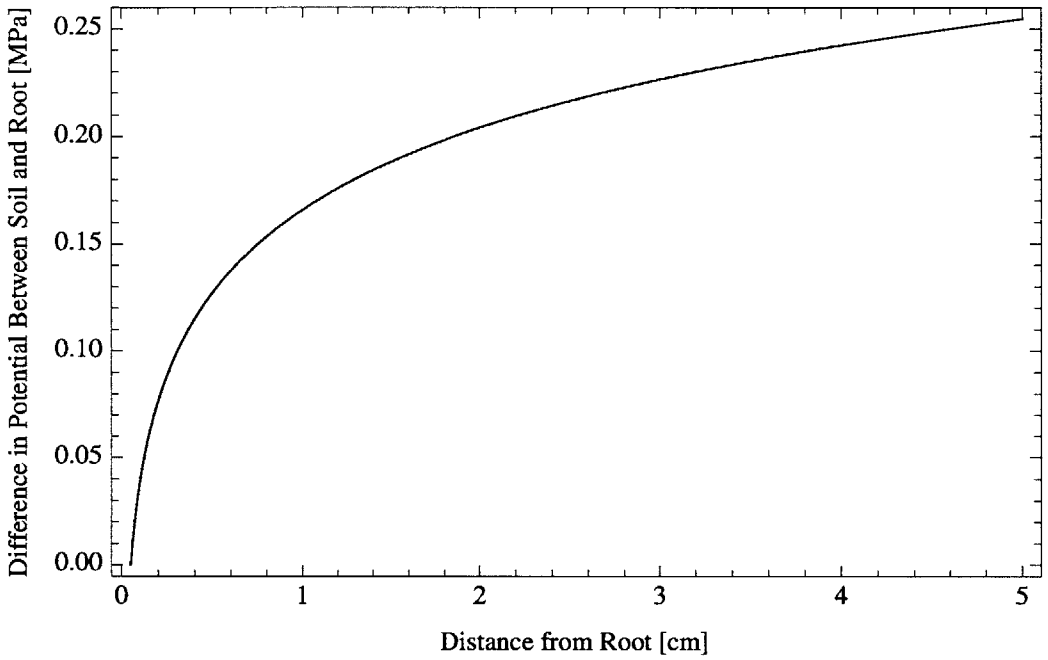

Figure 4-5: The difference in potential between the soil and root is shown as a function of radial distance for the simplified model of the root as a cylinder or radius 0.5 mm with constant flux per unit length.

to the water supply system.

Chapter 5

Modeling A Wick Irrigation System

To evaluate the feasibility of creating a wicking system that relies on the suction plants generate to provide low energy irrigation, a model of the wick-soil-plant system was developed based on the model of soil moisture dynamics proposed by Daly et al [11]. A model for a single plant and dripper is created, and then expanded to the acre scale system, with 120 branches, containing 120 drippers each, stemming off a main line. The acre scale system has the same parameters as discussed in the conventional irrigation section in Chapter 2 and presented in Table A.1.

5.1 Wicking for a Individual Plant

Looking at the individual plant system, an electrical circuit analogue of the water potential can be created by assuming the flow starts in the pipe, passes through the wick, at which point there are 3 parallel flow paths: evaporation from the soil, downward flow into the ground water system, or evapotranspiration through the soil and plant into the atmosphere [11]. Figure 5-1 shows the electrical analogy of these various flow paths. For simplicity, the wick is assumed to be saturated with constant

conductivity and the evaporation for the soil is taken to be constant and equal to the maximal evaporation rate per unit area. Representative values of the figures are presented in Table A.4. The downward flux of water into the soil is simply the hydraulic conductivity as a function of soil moisture content given by equation 3.8. The soil-plant-atmosphere system is represented by a number of resistors in series with variable resistances to reflect the change in conductivity as a function of water potential.

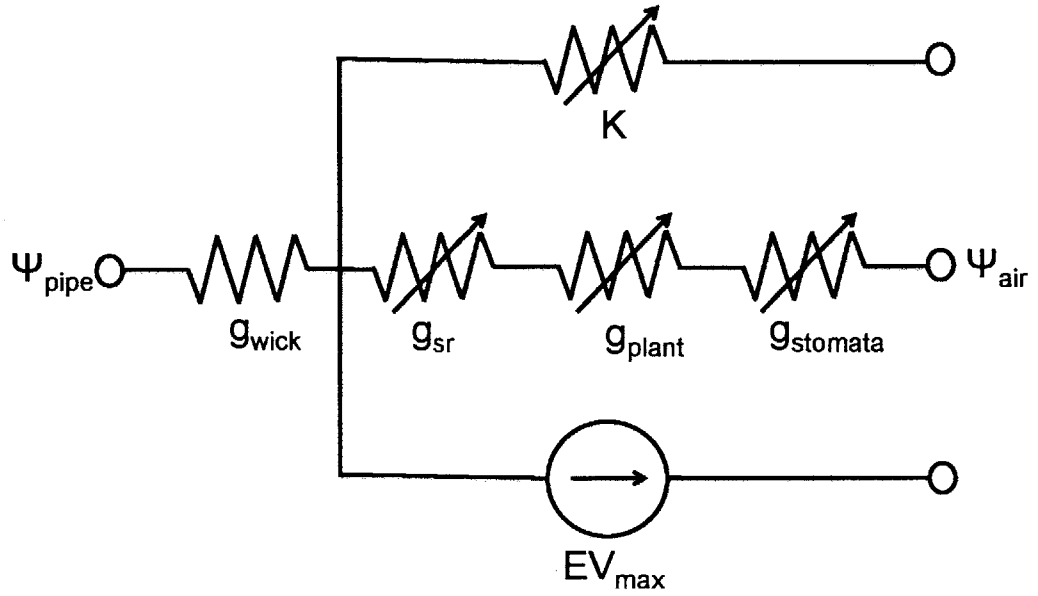

Figure 5-1: The flow of water from the pipe and through the wick can be compared to a circuit. Once the flow has exited the wick, there are 3 parallel paths it can take, downward into the soil, through the soil, roots, plant, and into the atmosphere, or straight evaporation from the soil. Downward flux, as well as the conductance of the soil-root system, plant, and stomata are modeled as variable resistors, while the evaporation rate from the soil is assumed to be constant.

The equilibrium operating point of the system is investigated, and as such, steady state is assumed with time dependence ignored. Under this restriction, the flow out

of the wick per unit area or irrigated land is defined by

$$w = \frac{W}{D_{dripper} D_{branch}} = EV_{plant} + EV_{max} + K \tag{5.1}$$

where W is the volumetric flow out of the wick, $D_{dripper}$ and D_{branch} give the spacing between drippers along a branch and between the branches themselves respectively, and hence define the ground surface area corresponding to each wick, EV_{max} is the maximum evaporation rate from soil, K is the downward water flux given by equation 3.8, and EV_{plant} is the evapotranspiration rate of the plant defined by equation 4.2, the Penman-Monteith equation [11]. Because equilibrium is being investigated, the saturation of the bulk soil is assumed to be constant, as the water leaving the wick either adsorbs into the plant through the roots, evaporates, or migrates downward into the soil.

The Darcy equation for the wick also gives the volumetric flowrate as a function of the difference in water potential between the pipe and bulk soil

$$W = g_{wick} \left(\Psi_{pipe} - \Psi_s \right) \tag{5.2}$$

where Ψ_{pipe} is the water potential of the pipe, Ψ_s is the water potential of the soil as a function of water content, defined by equation 3.6, and g_{wick} is the conductance of the wick. The wick conductance is assumed to be constant, and defined as

$$g_{wick} = \frac{K_{wick} A_{wick}}{\rho_w g L_{wick}} \tag{5.3}$$

where K_{wick} is the saturated conductivity, L_{wick} is the wick length, and A_{wick} is the cross-sectional area of the wick. Water is assumed to flow out of the wick only from the cross-sectional face, and not from the sides of the wick. The specifics of the wick design would dictate the amount of wick surface area exposed to the soil - here it is assumed that the wick is only exposed to soil at the tip. This assumption is made

to be a conservative estimate, as in actuality the area out of which the water would flow would be greater than the cross-sectional area, and hence the conductance would likewise be greater.

Similarly, the Darcy equation can be used to describe the flux of water through the soil, roots, and plant, as a function of the gradient in water potential between the soil and leaf. As evapotranspiration accounts for nearly all water flux through the plant, the Darcy equation for the soil-root-plant system can be approximately equated to the Penman-Monteith

$$EV_{plant} = g_{srp} (\Psi_s - \Psi_l) \tag{5.4}$$

where g_{srp} is the conductance per unit ground area of the soil-root-plant system. g_{srp} is the combined conductance of the in series soil-root conductance per unit area, g_{sr} from equation 4.6, and the plant conductance per leaf area, g_p from equation 4.5

$$g_{srp} = \frac{L_{AI} g_{sr} g_p}{g_{sr} + L_{AI} g_p} \tag{5.5}$$

where L_{AI} is the ratio of leaf area to ground area. While the soil-root conductance depends on the hydraulic conductivity and the average distance over which water travels to the root, equation 4.6 presents a simplified model by relating the average distance water travels to root depth, Z_r, and root area ratio R_{AI}. This model of soil-root conductance is simplified as in actuality the plant is dynamic. The drop in conductance associated withthe soil drying would be partially mitigated by root growth and decreases in the length scale over which water travels [11]. These responses, however, are not included in the model.

Equations 3.6, 4.2, 5.1, 5.2, and 5.4 form a system of 5 equations with 5 variables s, Ψ_l, Ψ_{pipe}, EV_{plant}, W. This system of equations is only applicable for the range over which Ψ_l is between Ψ_{wilt} and 0 Pa. At 0 Pa leaf potential, the soil is assumed to be at saturation, with essentially zero matric potential, and the flux of water through

the wick simply becomes a function of the water pressure in the pipe

$$\Delta Q = g_{wick}\Psi_{pipe} \tag{5.6}$$

For the parameters used in the model, and given in Tables A.1 - A.4, this occurs at a soil saturation of .92, and a pipe pressure in the irrigation system of 1.68 kPa.

While the nonlinearity of the system makes analytical solutions difficult, numerical solutions of the system of equations can be obtained by specifying an initial condition. Figures 5-2 through 5-5 show the numerically determined relations between the variables EV_{plant}, Ψ_l, Ψ_{pipe}, W, and s.

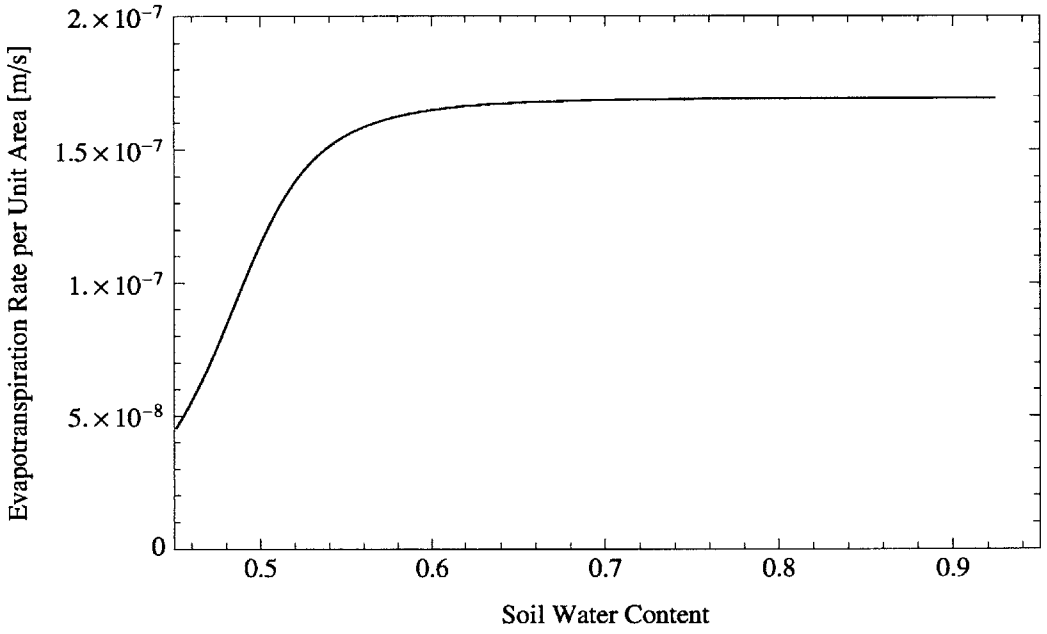

Figure 5-2: Evapotranspiration rate as a function of soil water content as determined by numerically solving the system of equations.

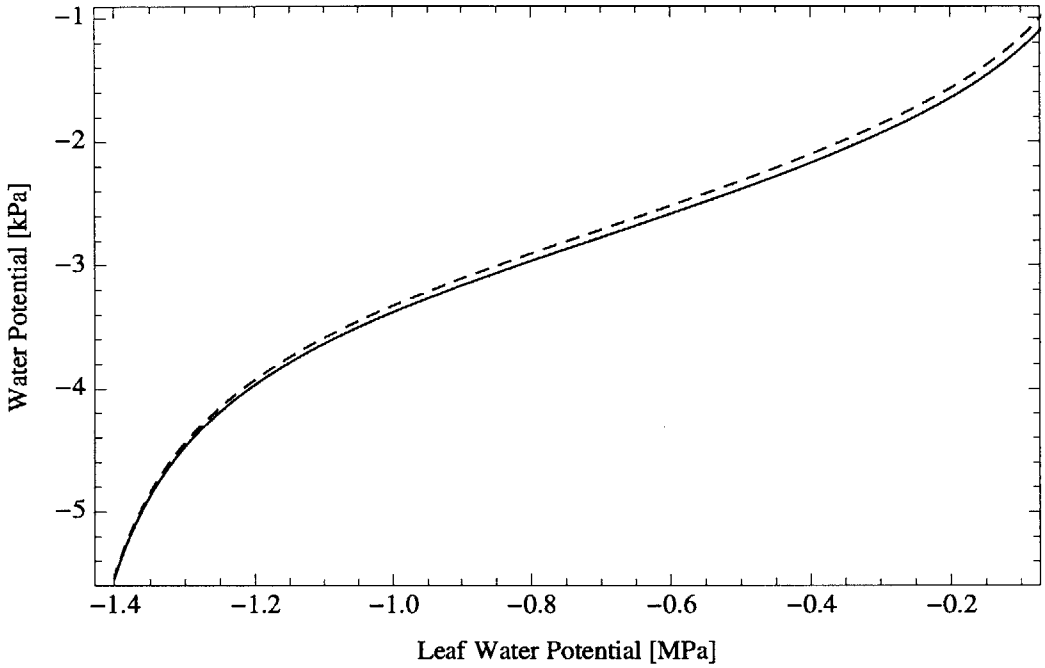

Figure 5-3: Water potential of the soil (solid) and pipe (dashed) is shown as a function of the leaf potential. As leaf potential increases, the potential drop between the pipe and soil increases due to the increase in flow rate through the wick.

5.2 Small-Scale Wicking Irrigation System

These results are expanded for the operation of a whole irrigation system with the same spacing parameters as in Chapter 2 - a $60m \times 60m$ system with 120 branches each containing 120 drippers. The pressure distribution and flow rates are determined by setting the leaf water potential of the final plant in the system and determining the potential at the end of the pipe. The pressure losses along the line between drippers are determined using the Darcy-Weisbach equations given by equation 2.1 and 2.3, and the system of equations is solved for each dripper using the water potential in the pipe as the initial condition. A representative value for the minor loss coefficient for the wicks in this system is taken to be equivalent to that of the drippers in the ideal and orifice system. For a leaf potential of the final plant set near the wilting point

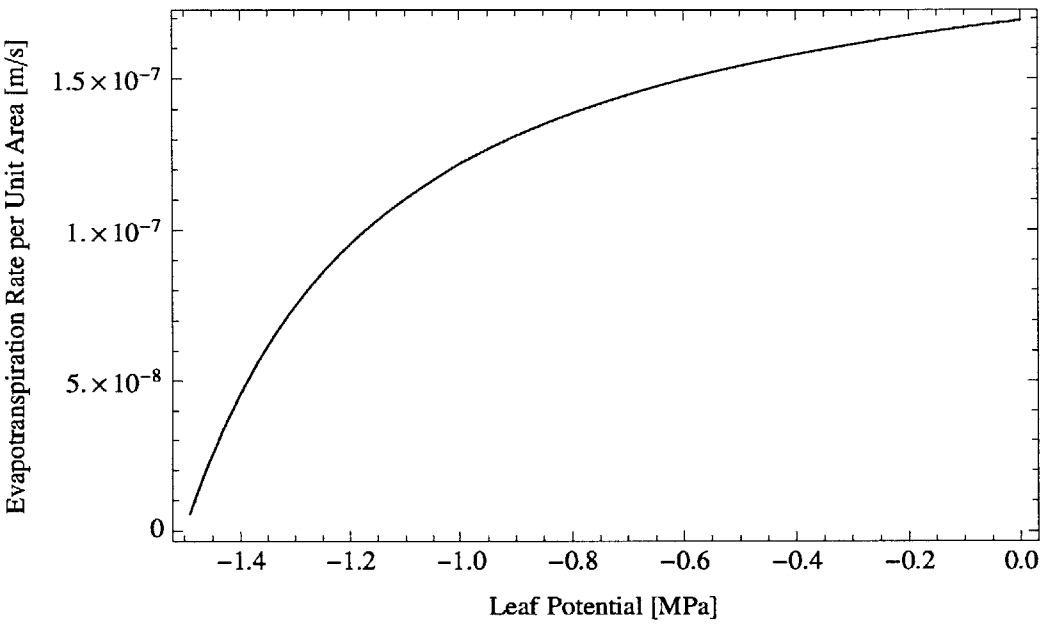

Figure 5-4: Evapotranspiration rate per unit area is given as a function of leaf potential as determined by the Penman-Monteith equation.

there would be no required input power. Rather, the negative power of the system indicates that, in theory, the flow of water through the irrigation system could be used as a power source. It is important to note that these results are for steady operating conditions, and that initially providing water to the wicks in the branches would require external power. These steady state operating conditions, however, result in a daily system flow rate of 12.9 $\frac{kL}{day}$, which is just more than half the desired daily flow rate of 25 $\frac{kL}{day}$. This leads to growing all the plants in a water stressed environment. The distribution of dripper flow rates and the pumping pressure in the line for a leaf potential in the final plant of $-1.1MPa$ are shown in Figures 5-6 and 5-7 respectively.

As the leaf potential of the final plant is raised, the amount of power the system generates decreases until eventually the system requires positive power to be supplied. Simultaneously, the daily flow rate of the system increases because the evapotranspiration rate increases with increasing leaf potential as shown in Figure 5-4. Thus, the

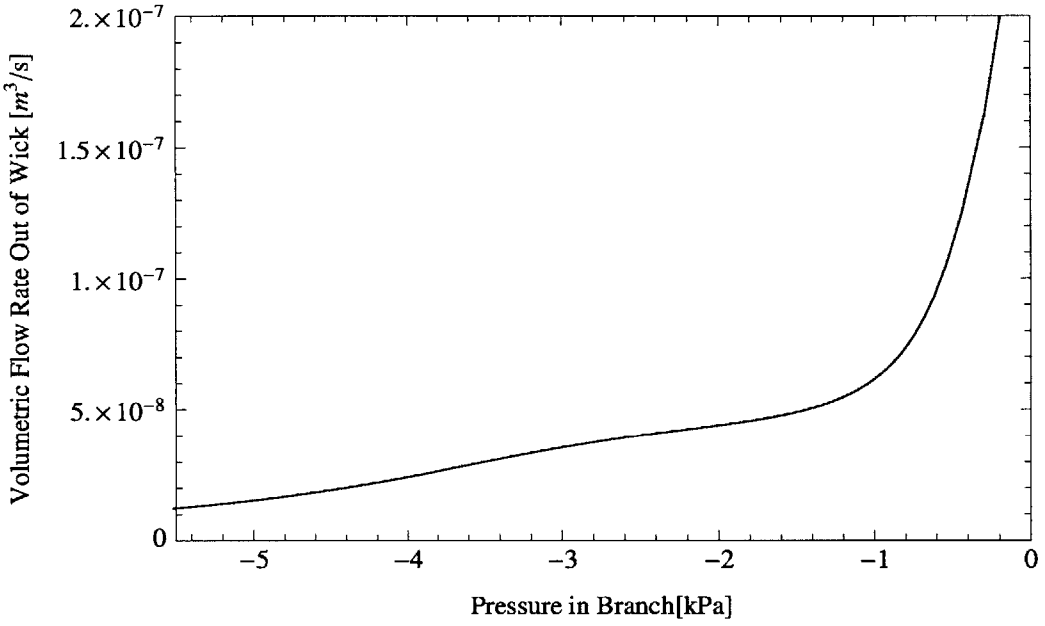

Figure 5-5: Flow rate out of the pipe is given as a function of pipe potential as determined by numerically solving the system of equations.

wick flow rate increases for each wick in the system. The distribution of flow rates of wicks in the system, however, also increases as greater disparities arise between the amount of water supplied by each wick. This results in some plants experiencing mild water stresses, while other plants are receiving an excess of water. Figure 5-8 shows the distribution of flow rates for the wicks in a system with a final leaf potential of $0.5MPa$, an input power of 0.2 W, and a daily system flow rate of 24.8 $\frac{kL}{day}$.

As illustrated in Figure 5-9, the Uniformity Coefficient of the system initially increases with an increase in the final leaf potential as the discrepancy between the desired flow rate and average wick flow rate decreases, masking the disparity in flow rates across the system. Further increases in leaf potential, however, no longer hide the disparity, and the Uniformity Coefficient drops. Figure 5-10 shows the power input as a function of daily flow rate required for the wicking system.

When designing a wicking system, balancing the power benefit of lower leaf po-

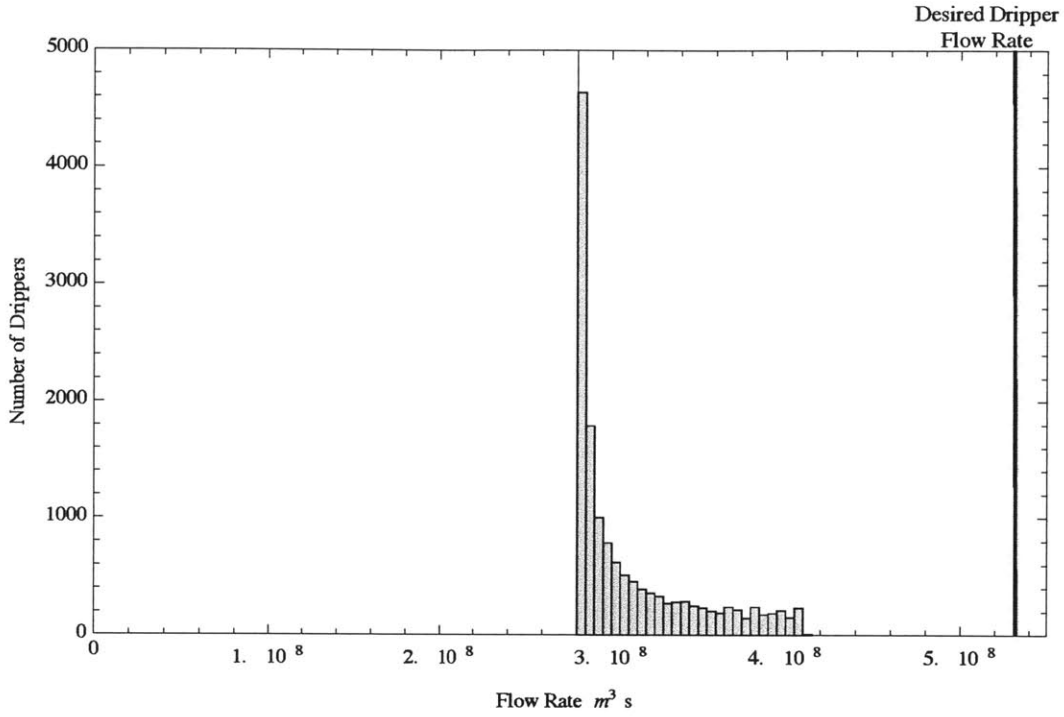

Figure 5-6: The distribution of dripper flow rates is illustrated for the case where the final leaf potential is set to $-1.1MPa$. The dark line shows the desired dripper flow rate necessary to provide 25,000 $\frac{L}{day}$ to the field.

tentials of the plants with the cost of limited flow rates is critical. Even as the leaf-potential of the final plant is raised, the distribution of flow rates out of each dripper increases, such that even if the system delivers the desired 25,000 $\frac{L}{day}$, individual plants experience a discrepancy in water supply. Plants near the end of the line suffer from a deficit of water, while water is supplied in excess to those near the start of the line.

While specific design considerations of the interface between the wick and the soil will impact the conductance of the wick, such as increasing wick area to increase hydraulic conductivity, the majority of the losses in the system come from the flow of water through the soil. Minimizing the distance water has to travel, by placing the wicks as close to plant roots as possible will help maximize the power benefit

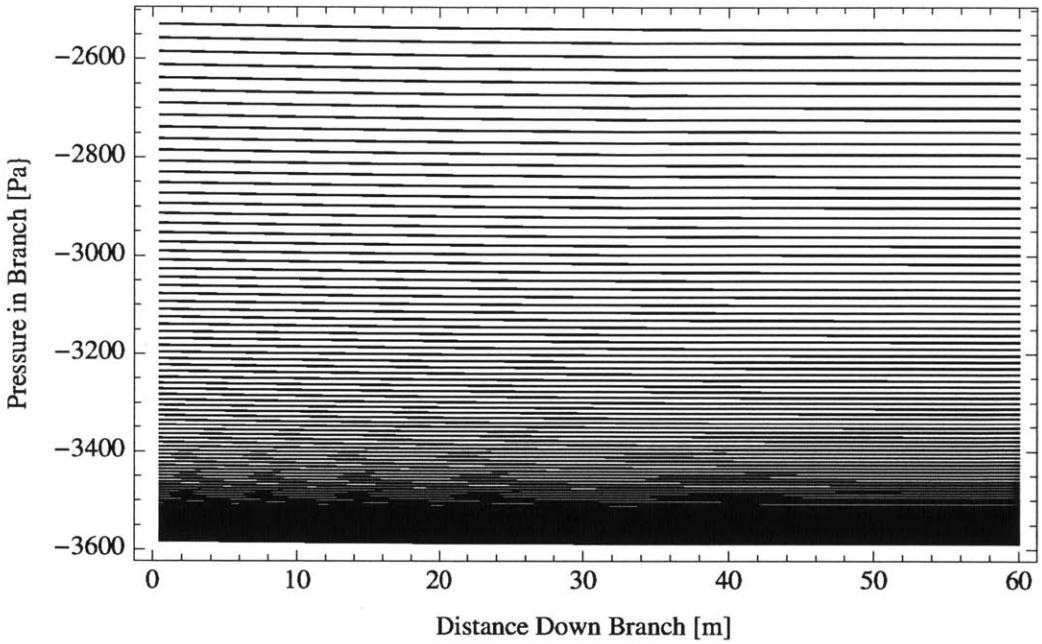

Figure 5-7: The pressure in each branch of the system is plotted as a function of distance down the branch for the case where the final leaf potential is set to $-1.1MPa$. Each line corresponds to an individual branch, with the top line illustrating the first branch, while the bottom line corresponds to the last branch in the system. While pressure drops along each branch, flow through the mainline of the system results in the largest pressure losses.

the system can achieve. As the plants are dynamic, the roots will tend to grow toward water sources helping to keep the distance water travels through the soil to a minimum. One concern, however, is designing a wick that prevents the roots from penetrating and clogging the branches of the irrigation system. If the roots are able to clog the line, then all downstream plants of the clog would be cut-off from the water.

In addition, the type of soil has a large impact on the performance of the system as the water retention curve and hydraulic conductivity varies greatly between soils. Soils with high matric potentials can not provide as great an energy benefit for a wicking system as those with extrememly negative matric potentials. In addition,

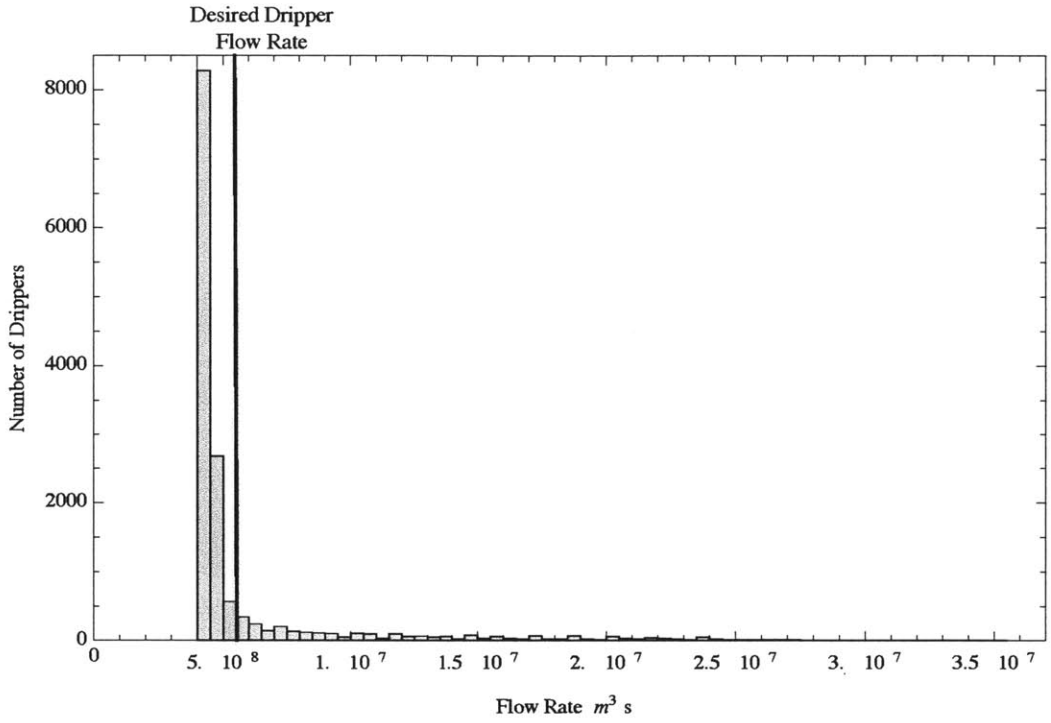

Figure 5-8: The distribution of dripper flow rates is illustrated for the case where the final leaf potential is set to $-0.5MPa$. The dark line shows the desired dripper flow rate necessary to provide 25,000 $\frac{L}{day}$ to the field.

the hydraulic conductivity of the soil has a large impact on the energy lost as the water travels to the plant. Soils with low hydraulic conductivity require greater water potential gradients to sustain the same rate of flux. The design of any wicking system would have to be carefully tuned to the specific soil type for each application.

5.3 Direct Root-Wick Coupling

In the wicking system described above, the matric potential of the soil provides the driving force behind the flow of water though the irrigation system. If the flux of water though the soil could be eliminated by developing a wick that coupled directly to the root, the large negative potentials at the root surface could provide a greater

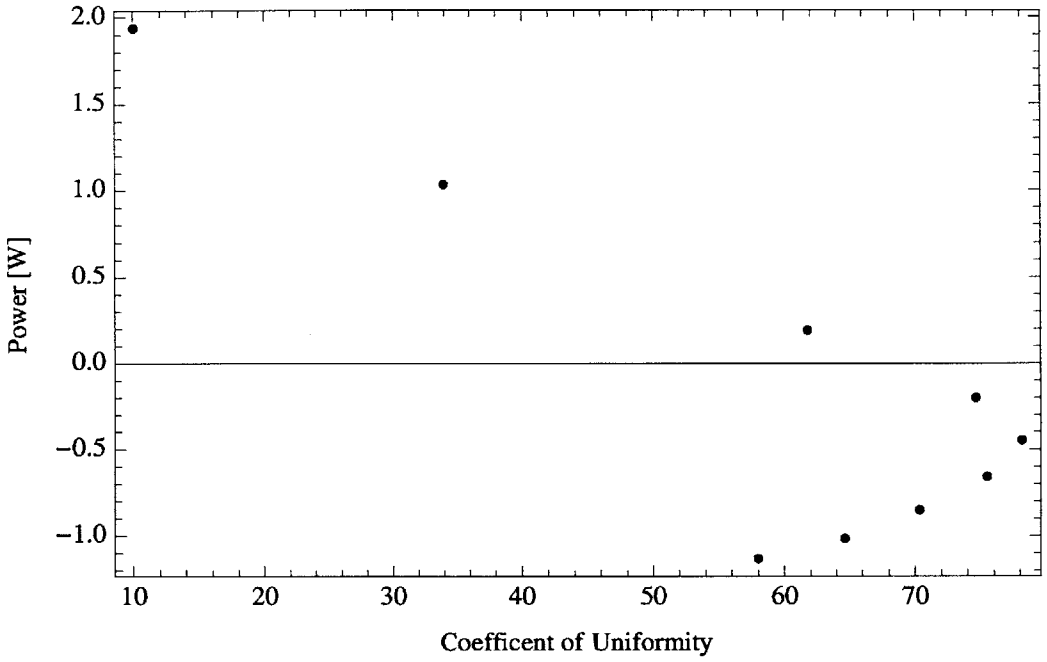

Figure 5-9: The Coefficent of Uniformity and power for the wicking system determined by numerically solving the system of equations for a given leaf potential of the final plant.

suction than that possible in the soil. This coupling would also minimize water losses due to downward water flux and surface evaporation by providing the water directly to the plant. Any implementation of this design, however, would need to look at the limit as to the amount of water a single root of the plant could adsorb. In the system discussed above, water was delivered to all of the plant's roots, however in the direct root coupling, there would be a large discrepancy between the roots directly coupled to the line receiving water, and those in the soil. It would be critical to investigate the limitations on a single root providing water to the whole plant. In addition, since the soil provides essential nutrients to the plant, investigation of the impacts of nutrient adsorption by the plant under such coupled root-wick irrigation conditions would be required.

For the direct coupling set-up, the water potential at the roots is taken to be equal

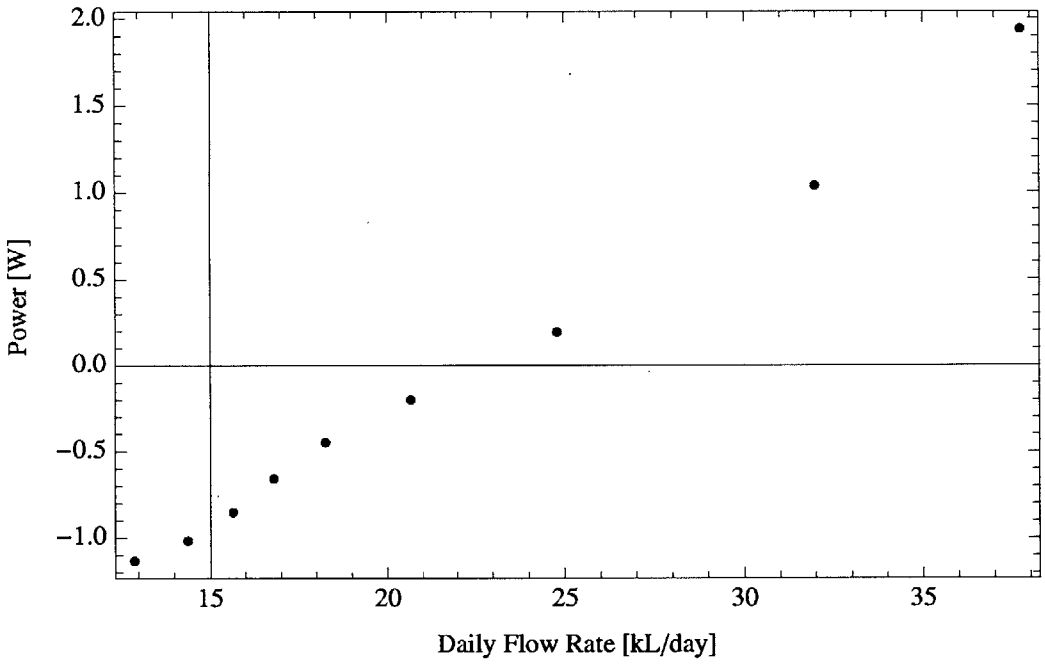

Figure 5-10: The input power of the wick system is shown as a function of daily flow rate. Compared to the orifice dripper, the wick can deliver more water with substantially less input power.

to the water potential in the leaf plus the potential lost due to the plant conductance given by

$$\Psi_{roots} = \Psi_l + \frac{EV_{plant}}{g_p} \tag{5.7}$$

The potential losses across the mechanical coupling between the wick and root depend largely on the wick design. As an estimate, the losses are assumed to be equal to that of the saturated wick used in the previously discussed system, giving a water potential in the pipe, as a function of leaf potential by

$$\Psi_{pipe} = \Psi_{roots} + \frac{D_{drippers} D_{branch} EV_{plant}}{g_{wick}} \tag{5.8}$$

This system has substantially less loss between the plant and pipe than in the case where the soil acts as an intermediate connection.

As above, the leaf water potential of the last plant in the line is specified, and the system of equations along with the Darcy-Weisbach equaions are solved to determine the pressure and flow profile of the system. By eliminating the potential losses associated with the soil, the system can generate substantially more power. Figure 5-11 shows the relationship between system flow rate and power for the system with mechanical coupling directly between the wick and root. The direct root-wick coupling experiences the same problems of variation between the water flux to individual plants as the wicking system in Section 5.2. In the case of the direct root coupling, however, waste water is minimized, as all water goes to the plant. In addition, the impact on soil type would be eliminated. Developing a direct root-wick coupled irrigation system could be applied more universally, although considerations for the differences between plant species would still be necessary.

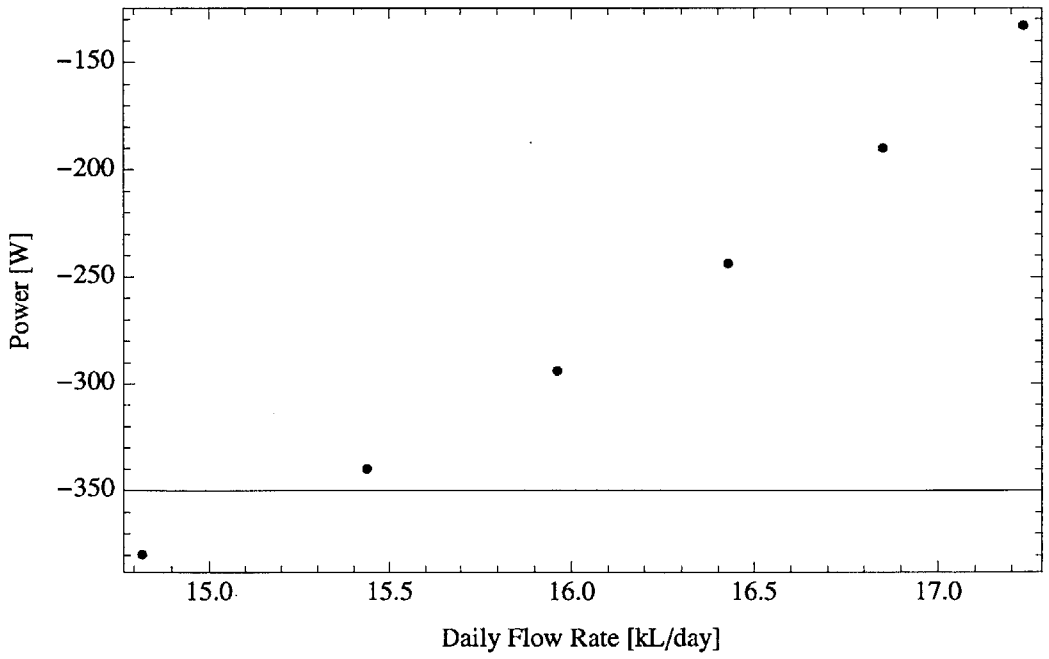

Figure 5-11: The input power of the direct root-wick coupled system is shown as a function of daily flow rate. Compared to the orifice dripper and regular wick system, this direct coupling could deliver water while simultaneously generating power, and eliminate losses to evaporation and downward flux into the soil.

Chapter 6

Conclusion

In theory, wicking systems hold the potential to substantially reduce the necessary pumping power required for irrigation, potentially even serving as a source of power generation. While a system that relies on both the negative water potential of soil as well as that of plants could provide reductions in irrigation power, creating a direct connection between the pipe and plant root would enable the use of large negative water potential at the root surface. Such a directly coupled system would provide the greatest power benefits, while minimizing water lost to soil evaporation and downward flux into the soil.

Questions as to the operation of such a system in an unsteady state still remain. While in equilibrium, a wicking system requires minimal to no input power, initially getting the system operating would still entail pumping the water through the line. In addition, while the system would be self-regulating following a rainstorm that saturates the field by reducing the flow rate of water through the system, the time-scale of this self-regulation needs to be investigated. Changes in response of the system to the natural variations in water uptake plants require throughout the growing stages would also need to be determined. The current investigation considers the system preformance at the point of maximum water requirements of the plant, yet earlier phases of growth also remain to be considered.

The actual improvements achieved by a wicking system would largely depend on the implementation and system design, but using the wicking power of plants to help power crop irrigation holds the potential to significantly reduce the power requirement and minimize water losses. Ensuring that roots don't grow into the wicks and clog the pipes would be a critical design problem any wicking system would need to address. The cost and durability of a wicking system would determine the success of implementation, but in terms of power and water efficiency, an irrigation method that relies on the principles of wicking could be a promising solution to the problem of micro-irrigation for subsistence farmers.

Appendix A

Tables

Table A.1: Irrigation System Parameters

Parameter	Value	Units	Description
$N_{branches}$	120		Number of branches in system
$M_{drippers}$	120		Number of drippers per branch
D_{branch}	0.5	m	Distance between branches
$D_{dripper}$	0.5	m	Distance between drippers
$Q_{system}^{desired}$	25,000	$\frac{L}{day}$	Desired daily flow rate for 1 acre irrigation system
q_{max}	5.36×10^{-8}	$\frac{m^3}{s}$	Flow rate of each dripper necessary to achieve $Q_{system}^{desired}$
d_{branch}	0.02	m	Diameter of branch
$d_{MainLine}$	0.05	m	Diameter of main line
g	9.8	$\frac{m}{s^2}$	Acceleration due to gravity
ρ_w	1000	$\frac{kg}{m^3}$	Density of water
μ	1×10^{-3}	Pa s	Viscosity of water
ϵ	1.5×10^{-6}		Roughness coefficient of pipe
$\kappa_{dripper}$	0.22		Minor loss coefficient of dripper - estimated from minor losses due to expansion and contraction of flow [21]
κ_{branch}	0.8		Minor loss coefficient due to t-junction for branch out of the main line [21]
P_{ideal}	1.98	W	Theoretical minimum power of required to overcome friction in system

Table A.2: Soil Parameters for Loamy Sand Used in Model [11]

Parameter	Value	Units	Description
K_{sat}	100	$\frac{cm}{day}$	Saturated hydraulic conductivity
$\bar{\Psi}_s$	-0.17×10^{-3}	MPa	Soil water potential at saturation
b	4.38		Empirically determined exponent of the retention curve
n	0.42		Porosity of soil

Table A.3: Parameter values used in soil-root-plant-atmosphere model

Parameter	Value	Units	Description
T	25	C	Ambient temperature
% Relative Humidity	50	%	Average relative humidity in India [2]
Δ	145.4	$\frac{Pa}{K}$	Rate of change of vapor pressure with temperature
δ	1580.35	Pa	Vapor pressure deficit
R_n	500	$\frac{W}{m^2}$	Net irradiance reaching leaf [11]
ρ_a	1.2	$\frac{kg}{m^3}$	Density of air
c_p	1012	$\frac{J}{kgK}$	Specific heat of air
λ_v	2.5×10^6	$\frac{J}{kg}$	Latent heat of water vaporization
γ	66	$\frac{Pa}{K}$	Psychrometric constant
g_a	2×10^{-2}	$\frac{m}{s}$	Atmospheric conductance [11]
g_{pmax}	1.17×10^{-11}	$\frac{m}{s}$	Maximum conductance of plant [11]
g_{smax}	2.5×10^{-2}	$\frac{m}{s}$	Maximum conductance of stomata [11]
Ψ_{lo}	-0.05	MPa	Leaf potential at which stomata start to close [11]
Ψ_{wilt}	-1.5	MPa	Leaf potential at which plant wilts [18]
c	2		Parameter of vulnerability curve [11]
d	2×10^6	Pa	Parameter of vulnerability curve [11]
R_{AI}	1		Ratio of root area to ground area
Z_r	1	m	Root length

Table A.4: Parameter values used in wicking system model

Parameter	Value	Units	Description
EV_{max}	2.3×10^{-9}	$\frac{m}{s}$	Maximum evaporation rate from the soil per unit area [11]
K_{wick}	2.3×10^{-3}	$\frac{m}{s}$	Hydraulic conductivity of fiberglass wick at saturation [15]
A_{wick}	7.85×10^{-5}	m^2	Cross-sectional area of wick
L_{wick}	0.03	m	Wick length
L_{AI}	4		Ratio of leaf area to ground area [6]

Bibliography

[1] Boeing subsidiary spectrolab sets world record for solar cell efficiency. http://boeing.mediaroom.com/index.php?s=43item=2645

[2] India.

[3] J-SC-PC Plus Emitters. http://www.jains.com/irrigation/emitters

[4] Water Scarciy. http://www.un.org/waterforlifedecade/scarcity.shtml

[5] SimSphere Workbook: Chapter 10, August 2003. https://courseware.e-education.psu.edu/simsphere/workbook/ch10.html

[6] R.G. Allen, L.S. Pereira, D. Raes, and M. Smith. Crop evapotranspiration - guidelines for computing crop water requirements. Irrigation and drainage paper 56, Food and agriculture organization of the united nations, 1998.

[7] World Bank. Addressing the electricity gap. Technical report, World Bank, June 2010.

[8] World Bank. Deep wells and prudence: towards pragmatic action for addressing groundwater overexploitation in India. Technical report, World Bank, 2010.

[9] J. Bear. *Dynamics of fluids in porous media.* American Elsevier Pub. Co., 1972.

[10] R.B. Clapp and G.M. Hornberger. Empirical equations for some soil hydraulic properties. *Water resources research*, 14(4):601–604, 1978.

[11] E. Daly, A. Porporato, and I. Rodriguez-Iturbe. Coupled dynamics of photosynthesis, transpiration, and soil water balance. Part I: Upscaling from Hourly to Daily Level. *Journal of hydrometeorology*, 5:546–558, 2004.

[12] V. Demir, H. Yurdem, and A. Degirmencioglu. Development of prediction models for friction losses in drip irrigation laterals equipped with integrated in-line and on-line emitters using dimensional analysis. *Biosystems Engineering*, 96(4):617–631, 2007.

[13] I. Hussain and M.A. Hanjra. Irrigation and poverty alleviation: Review of the empirical evidence. *Irrigation and drainage*, 53:1–15, 2005.

[14] S.J. Keller. Mapping underground water sources for drip irrigation could change African village life, says Stanford researchers, December 2011. http://news.stanford.edu/news/2011/december/solar-drip-irrigation-120511.html

[15] J.H. Knutson and J.S. Selker. Unsaturated hydraulic conductivities of fiberglass wicks and designing capillary wick pore-water samplers. *Soil science society of america journal*, 58:721–729, May-June 1994.

[16] G. Kopp and J.L. Lean. A new, lower value of total solar irradiance: Evidence and climate significance. *Geophysical research letters*, 38, 2011.

[17] B.E. Livingston. Plant water relations. *The quarterly review of biology*, 2(4):494–515, Dec. 1927.

[18] P.S. Nobel. *Physicochemical and environmental plant physiology.* Elsevier Academic Press, 4th edition, 2009.

[19] T. Sauer, P. Havlik, U.A. Schneider, E. Schmid, G. Kindermann, and M. Obersteiner. Agriculture and resource availability in a changing world: the role of irrigation. *Water resources research*, 46(6), June 2010.

[20] J.S. Sperry, F.R. Adler, G.S. Campbell, and J.P. Comstock. Limitation of plant water use by rhizosphere and xylem conductance: results from a model. *Plant, cell and environment*, 21:347–359, 1998.

[21] F.M. White. *Fluid mechanics.* McGraw Hill, 7th edition, 2011.